AAS 00-166

Shoot the Moon[ϰ]

Wang Sang Koon[†], Martin W. Lo[*], Jerrold E. Marsden[†], Shane D. Ross[†]

Abstract

In 1991, the Japanese Hiten mission used a low energy transfer with a ballistic capture at the Moon which required less ΔV than a standard Hohmann transfer to the Moon. In this paper, we apply the same dynamical systems techniques used to produce the "Petit Grand Tour" of Jovian moons to reproduce a Hiten-like mission. We decouple the Sun-Earth-Moon-Spacecraft 4-body problem into two 3-body problems. Using the invariant manifold theory of the Lagrange points of the 3-body systems, we are able to construct low energy transfer trajectories from the Earth and ballistic capture trajectories at the Moon. The techniques used in the design and construction of this trajectory may be applied in many situations.

1. Introduction

In this paper, we apply the same dynamical systems techniques used to produce the "Petit Grand Tour" of Jovian moons to reproduce a Hiten-like mission (Ref. 1). In 1991, the Japanese Hiten mission used a low energy transfer with a ballistic capture at the Moon based on the work of Belbruno and Miller (Ref. 2) on the Weak Stability Boundary theory (WSB). Discussions at the "Advances in Nonlinear Astrodynamics Conference" in 1993 (Ref. 3) produced the generally-accpeted view that the WSB is generated by the invariant manifold structure of the Lagrange points of the Sun-Earth and Earth-Moon systems. Belbruno documents his conjectures on the structure of the WSB in Ref. 4.

The three key ideas of our approach to "Shoot the Moon" are:

1.) Treat the Sun-Earth-Moon-Spacecraft 4-body problem as two coupled circular restricted 3-body problems, Sun-Earth and Earth-Moon systems;
2.) Use the unstable manifolds of periodic orbits about the Sun-Earth Lagrange points to provide a low energy transfer from Earth to the stable manifolds of periodic orbits around the Earth-Moon Lagrange points;
3.) Use the stable manifolds of the periodic orbits around the Earth-Moon Lagrange points to provide a ballistic capture about the Moon.

We start with the planar circular restricted 3-body problem (PCR3BP) to compute the invariant manifolds. The final trajectory starting from the Earth and ending in lunar capture is integrated in the Bi-Circular Problem (BiCP) where both the Moon and the Earth are assumed to move in circular orbits in the Ecliptic, and the spacecraft is an infinitesimal mass point.

The final Bi-Circular solution has been differentially corrected to a fully integrated trajectory with JPL ephemeris using JPL's LTool (Libration Point Mission Design Tool). LTool is JPL's new

---

[ϰ] A New Technolgoy Report has been filed at JPL on the work reported in this paper.

[†] Control and Dynamical Systems, California Institute of Technology, Pasadena, CA 91125

[*] Navigation and Mission Design, Jet Propulsion Laboratory, California Institute of Technology, Pasadena, CA 91109. The communicating author may be reached at Martin.Lo@jpl.nasa.gov

mission design tool currently under development, based on dynamical systems theory. This will be described in a subsequent paper.

2. The Three Body Problem

We start with the PCR3BP as our first model of the mission design space, the equations of motion for which in rotating frame with normalized coordinates are:

$$x'' - 2y' = \Omega_x, \quad y'' + 2x' = \Omega_y, \tag{1}$$

$$\Omega = \frac{x^2 + y^2}{2} + \frac{1-\mu}{r_1} + \frac{\mu}{r_2}.$$

The subscripts of Ω denote partial differentiation in the variable and apostrophes after the variables are time derivatives. The variables r_1, r_2, are the distances from (x,y) to the Sun and Planet respectively. See Szebehely's classic text (Ref 5.) for an excellent derivation and description.

The coordinates of the equations use standard PCR3BP conventions: the sum of the mass of the Sun and the Planet is normalized to 1 with the mass of the Planet set to μ; the distance between the Sun and the Planet is normalized to 1; and the angular velocity of the Planet around the Sun is normalized to 1. Hence in this model, the Planet is moving around the Sun in a circular orbit with period 2π. The rotating coordinates, following standard astrodynamic conventions, are defined as follows: the origin is set at the Sun-Planet barycenter; the x-axis is defined by the Sun-Planet line with the Planet on the positive x-axis; the xy-plane is the plane of the orbit of the Planet around the Sun (see Figure 1).

Figure 1. The 3 Body Problem in Rotating Coordinates.

Although the PCR3BP has 3 collinear libration points which are unstable, for the cases of interest in this paper, we examine only L_1 and L_2. These equations are autonomous and can be put into Hamiltonian form with 2 degrees of freedom. It has an energy integral called the Jacobi constant which provides 3 dimensional energy level surfaces:

$$C = (x'^2 + y'^2) - 2\Omega(x,y). \tag{2}$$

The power of dynamical systems theory is that it is able to provide additional structures within the energy surface to characterize the different regimes of motions.

2.1 Orbit Classes Near L_1 and L_2

The work of Lo and Ross (Ref. 6) demonstrated that the dynamics of the L_1 and L_2 region is extremely important for the understanding of many disparate dynamical phenomena in the Solar System and also for space mission design. In order to better understand the dynamics of this region, we now review the work of Conley (Ref. 7) and McGehee (Ref. 8) which provides an essential characterization of the orbital structure near L_1 and L_2. McGehee also proved the existence of homoclinic orbits in the Interior Region. Llibre, Martinez, and Simo (Ref. 9) computed homoclinic orbits of L_1 in the Interior Region. They further extended McGehee's results and proved a theorem using symbolic dynamics for orbital motions in the Interior Region. One of the key results in Koon et al. (Ref. 1) is the completion of this picture with the computation of heteroclinic cycles in the Planet Region between L_1 and L_2. We will refer to the various regions by the following short hand: S for the Interior Region which contains the Primary Mass, J for the Region which contains the Secondary Mass, X for the Exterior Region outside the Secondary Mass' orbit. For the Sun-Earth system, S represents the Sun and J represents the Earth. For the Earth-Moon system, S represents the Earth and J represents the Moon.

Figure 2 below schematically summarizes the key results of Conley and McGehee. The Hill Region is the projection of the energy surface from the phase space onto the configuration space, the xy-plane. Figure 2a shows the Hill Region for an energy value just about that of L_2, represented by the white space. The grey region is energetically forbidden. In other words, with the given energy, our spacecraft can only explore the white region. More energy is required to enter the grey Forbidden Region.

Figure 2a. The Hills Region Connecting the Interior Region (S), the Planet Region (J), and the Exterior Region (X).
2b. Expanded View of the L_2 Region with 4 Major Classes of Orbits.

Figure 2b is a blows-up of the L_2 Region to indicate the existence of four different classes of orbits. The first class is a single periodic orbit with the given energy, the planar Lyapunov orbit around L_2. The second class represented by a Green spiral is an asymptotic orbit winding onto the periodic orbit. This is an orbit on the stable manifold of the Lyapunov orbit. Similarly, although not shown, are orbits which wind off the Lyapunov orbit to form its unstable manifold. The third class, represented by red orbits, are transit orbits which pass through the J Region between the S and X Regions. Lastly, the fourth class, in blue, consists of orbits which are trapped in the S or X Regions. Note that orbits trapped in the region may be only temporarily captured although the duration may be very long.

2.2 Invariant Manifolds of Unstable Periodic Orbits

Let us examine the stable and unstable manifold of a Lyapunov orbit as shown in Figure 3 below. Of course, only a very small portion of the manifolds are plotted. Note the X-pattern typical of a saddle energy surface formed by the manifolds.

Figure 3. The Stable and Unstable Manifold of a Lyapunov Orbit.

Since the energy surface is 3-dimensional, this means that the 2-dimensional tubes of the manifolds of the Lyapunov orbits are separatrices! By this we mean the tubes separate different regimes of motion within the energy surface. Referring back to the schematic diagram, Figure 2b, we notice that the Red Transit Orbits pass through the oval of the Lyapunov orbit. This is no accident, but an essential feature of the dynamics on the energy surface. Lo and Ross (Ref. 6) referred to L_1 and L_2 as *gate keepers* on the trajectories, since the Jupiter comets must transit between the X and S regions through the J region and always seem to pass by L_1 and L_2. Chodas and Yeomans (Ref. 10) noticed that the comet Shoemaker-Levy9 passed by L_2 before it crashed into Jupiter. These tubes are the only means of transit between the different regions in the energy surface! In fact, all this was already known to Conley and McGehee some 3 decades ago.

The series of papers we referenced, starting with Conley's work, is a beautiful case study of the migration of abstract theory to concrete engineering applications. In fact, some of the work of Conley's group was funded by NASA in the 1960's during the Moon Race. It has taken some 30 odd years for that migration to occur. This was one of NASA and NSF's long-term investments that is now realizing its payoff inreal space mission applications.

2.3 Coupled Three Body Systems

The study of Hiten-like transfers requires four bodies: the Sun, Earth, Moon, and spacecraft. However, the structure of the phase space of the 4-body problem is poorly understood in comparison with the 3-body problem. By decomposing the 4-body problem into two 3-body problems, all of the machinery of 3-body invariant manifold theory becomes available. This is similar to the more standard approach in astronomy where the Solar System is viewed as a series of 2-body problems where Keplerian theory applies. JPL's spectacular multiple flyby missions such as Voyager and Galileo are based on this Keplerian decomposition of the Solar

System. But, when we want to use halo orbits and their invariant manifolds, a 3-body decomposition of the Solar System is natural. This, in effect, is what was done to design the "Petit Grand Tour" in Koon et al. (Ref. 1 and 11).

However, the success of this approach depends greatly on the particular 4 bodies. In order for low energy transfers to take place, the invariant manifold structures of the two 3-body systems must intersect within a reasonable period. Otherwise, the transfer may require an impractically long waiting period. For the Sun-Earth-Moon-Spacecraft case, this is not a problem. The invariant manifold structures of the Earth-Moon L_2 grow very quickly (on the order of 1 month) into the circular region around the Earth with a radius around 1,000,000 km. Similarly, the invariant manifold structures of the Sun-Earth L_1 and L_2 also extend quickly (on the order of 1 month) into the same circular region (1,000,000 km radius) around the Earth. The overlapping of these invariant manifold structures provide the low energy transfers between the Earth and the Moon. This explains why many of the techniques based on the WSB theory always aim for approximately 1,000,000 km away from the Earth as a starting point for the construction of the trajectory.

The invariant manifold structures of the Lagrange points are truly a network of dynamic super highways within the Solar System. If the invariant manifolds of the coupled 3-body systems intersect, then a low-energy transfer is possible. If their manifolds do not intersect, then a low-energy transfer is difficult to achieve. Notice, non-intersection does not imply impossibility of transfer. This is because transport via intersecting invariant manifolds is merely one of several transport mechanisms within the Solar System. For example, the manifolds of the Sun-Earth and Sun-Mars systems do not intersect even after more than 1,000,000 years of integration. Yet, transport between Mars and Earth are known to occur on a shorter time scale. This transport is due to secular resonances, another powerful and complex transport mechanism within the Solar System.

3. Earth-Moon Transfer Mechanism

3.1 Compute the 200 km Altitude Launch Point

To effect the Earth-Moon transfer, we must compute a Sun-Earth manifold which leaves the vicinity of the Earth toward the region of the Earth-Moon manifolds. To generate the manifolds, we must first produce Lyapunov orbits around the Lagrange points. For the Sun-Earth manifold, we select an L_2 Lyapunov orbit. An L_1 Lyapunov orbit is equally valid for this application. Figure 4a shows the Lyapunov orbit and a portion of its unstable manifold (red). The trajectories on the manifold were integrated until they hit the line labeled $\boldsymbol{\theta_{SE}}$. This is where we chose to compute the Poincare section in the variables { r, dr/dt } as shown in Figure 4b, where $r^2 = x^2 + y^2$. The Poincare section is the intersection of the trajectory with a hyperplane which is transversal (not parallel) to the trajectory in the energy surface. Since the planar problem has two degrees of freedom, its energy surfaces are 3-dimensional. Hence, the hyperplane in the energy surface is just a 2-dimensional plane. In this instance, we chose the { r, dr/dt } – plane because we want a manifold which approaches Earth as closely as possible since we want to use the manifolds of this Lyapunov orbit to leave the Earth. As the unstable manifold of the L_2 Lyapunov orbit is a tube, its Poincare section must be a distorted ellipse.

Figure 4. Sun-Earth Unstable Manifold and Poincare Section.

From Conely and McGehee's characterization of the orbital classes in the Earth-region between L_1 and L_2, summarized in Section 2.1, we know that any point within the ellipse of the Poincare section with the same Jacobi constant as the manifold must come from the Exterior Region outside of the Earth's orbit. Since we are trying to find an orbit that leaves the Earth and goes to the Moon, clearly, it cannot come from this region within the ellipse. However, by the same argument, points outside the red ellipse with the same Jacobi constant must come from the inside of the Earth Region. From experience, we know also that points near the manifold tend to stay

close to the manifold for a considerable amount of time. The closer a point is to the manifold, the longer it tends to linger near the manifold. Let us examine the behavior of points near the manifold by taking a small segment $[q_1, q_2]$ as indicated in Figure 5. Note that Figure 5 is the Poincare section of both the stable (green) and unstable (red) manifolds of the Lyapunov orbit. In this instance, the section was taken at $x = 1 - \mu$, using the { y, dy/dt } – plane. The point q_1 lies on the unstable manifold. All of the points in the segment have the same x-variable. We also require that they have the same energy which completely determines their phase space coordinates. The blue line schematically indicates the location of the Earth's postion in y, taking into consideration the Earth's finite size. But the dy/dt portion of the blue line has no meaning.

Figure 5. Using the Poincare Section to Find the Transfer Trajectory.

From the general theory described in Koon et al (Ref. 1), it is known that the points in the $[q_1, q_2]$ – segment will wind around the eqilibrium point, L_2, for different number of revolutions when integrated backwards. Theoretically, the point q_1 should wind around L_2 infinitely many times because it is on the unstable manifold which when integrated backwards winds onto the Lyapunov orbit. Whereas the point q_2, if it is sufficiently close to the unstable manifold, will wind around L_2 for a few revolutions. Then it will leave the L_2 vicinity guided by the stable manifold (integrating backwards) back near the Earth, since q_2 lies outside of the red ellipse.

Let us integrate the segment backwards and plot its pre-image on he Poincare section. Let P denote the Poincare map, and P^{-1} its inverse. $P^{-1}[q_1, q_2]$ is plotted in black and winds around the Poincare section of the stable manifold as predicted. Note $P^{-1}(q_1)$ is almost right on the stable manifold. Theoretically, $P^{-1}(q_1)$ should be exactly on the Lyapunov orbit. However, since all our computations are numerical approximations with finite precision, we should think of q_1 only as a point very close to the unstable manifold. Note in particular, that by the slightest change in the dy/dt parameter (or a small ΔV), we can move $P^{-1}(q)$ anywhere near Poincare section of the stable manifold in Figure 5. In this way, we can pick it to be exactly 200 km away from the Earth since {x, y, dy/dt} are determined by this process and dx/dt is determined from the Jacobi constant.

What will it do? In the time-reversed system, it must follow the "unstable manifold" of the time-reversed system to leave the Lyapunov orbit. But, that is just the stable manifold of the time-forward system. Since we picked the manifold very close to Earth as can be seen in Figure 4.a, one of the points in the $[q_1, q_2]$-segment must approach Earth along the stable manifold when integrated backwards. Let us integrate the segment backwards and plot the Poincare section and see just where these points come from with respect to the stable manifold. Let P denote the Poincare map, and P^{-1} its inverse. $P^{-1}[q_1, q_2]$ is plotted in black and winds around the Poincare section of the stable manifold as predicted. Note $P^{-1}(q_1)$ is almost right on the stable manifold. Theoretically, $P^{-1}(q_1)$ should be exactly on the Lyapunov orbit. However, since all our computations are numerical approximations with finite precision, we should think of q_1 only as a point very close to the unstable manifold. Note in particular, that by the slightest change in the dy/dt parameter (or a small ΔV), we can move $P^{-1}(q)$ anywhere on the stable manifold's Poincare section in Figure 5. In this way, we can pick it to be exactly 200 km away from the Earth since {x, y, dy/dt} are determined by this process and dx/dt is determined from the Jacobi constant.

3.2 Compute the Earth-Moon Transfer Point

Next we must compute obtain a trajectory to approach the Moon. Since the unstable manifold of the Sun-Earth Lyapunov orbit will move the spacecraft away from Earth into the Sun-Earth L_1 and L_2 region which is outside of the Moon's orbit, this suggests we need to use the Earth-Moon L_2 invariant manifold complex to effect the transfer to the Moon and eventual capture. In Figure 6, we show the stable manifold (green) of an Earth-Moon Lyapunov orbit and its Poincare section. Again from the Conley's classification theory, we know that any point within the green ellipse of the Poincare section of the stable manifold which has the same Jacobi constant as the manifold itself, must, by theory, be transported into the lunar region between the Earth-Moon's L_1 and L_2.

Figure 6. The Stable Manifold of the Earth-Moon L_2 Lyapunov Orbit and Its Poincare Section.

In Figure 7, we plot the Sun-Earth (red) and Earth-moon (green) Poincare sections. If we pick points outside of but close to the red ellipse, we can find a trajectory which departs at 200 km altitude from the Earth using the algorithm of Section 2.1. If we now also require this point to fall within the green ellipse, it is guaranteed to approach the Moon by the above argument.

Figure 7. The Poincare Sections of the Sun-Earth and Earth-Moon Manifolds.

There are several subtle and complex issues here. First of all, these Poincare sections were computed in "different rotating coordinate systems"! If one were to plot the Earth-Moon manifold in the Sun-Earth rotating frame, it would unravel into a mess. The use of the Poincare section avoided this mess, but, it introduced a phase. However, since each point on the Earth-Moon Poincare section requires different amounts of time to approach the Lyapunov orbit, there already is a nonlinear phasing issue in the Earth-Moon rotating frame.

A second issue is that fact that these manifolds are based on 3-body models. But, the trajectory we desire is based on 4-body models. Hence the initial conditions computed using this method may fail as the 4-body perturbations will "move" the ellipses of the Poincare sections slightly. However, using points nearby, a suitable solution can be found. A better approach is to recompute the Lyapunov orbits and their manifolds in the 4-body model desired. Then compute the Poincare sections to produce the orbit.

Third, since the energies of the Sun-Earth and Earth-Moon manifolds differ, the intersections produced in this manner require a small ΔV. By selecting the energies properly so that they match in both systems, this small ΔV may be eliminated. In other words, a completely free transfer after launch from Earth to lunar capture is possible!

The fact that these ΔV's are small and may even be eliminated can be seen from this well-known fact. From a 200 km circular orbit around the Earth, it requires approximately 3150 m/s of ΔV to reach the Earth-Moon L_1 or L_2. For another 50 m/s, you can reach the Sun-Earth L_1 or L_2! In other words, the Lyapunov orbits, halo orbits, and their invariant manifolds all have about the same energy on top of being colocated at roughly 1,000,000 km from the Earth! This happy set of coincidences is what enables these low energy lunar transfer and capture orbits. Given another 4-body system with different parameters, such transfers may not be available. Of course, when there are too many coincidences, often another phenomenon is at play, waiting to be discovered.

4. The Capture Mechanism

Let us now address the capture mechanism. Koon et al (Ref. 1, 11) provided the dynamical explanation and numerical algorithm for how these low energy captures occur. Once the spacecraft enters the green tube of the exterior stable manifold of the Earth-Moon L_2 Lyapunov orbit, it must go into the lunar region between the Earth-Moon L_1 and L_2. In order for this orbit to then leave the lunar region, it must leave via the interior stable manifolds of the L_1 Lyapunov orbit of the exact same Jacobi constant! Recall from Conley's classification, for each energy, there is exactly one Lyapunov orbit at L_1 and L_2 with the same energy. Hence all orbits which enter and leave the lunar region via a Lyapunov orbit at L_2 must depart via a Lyapunov orbit with the same energy at L_1. For this to occur, the Poincare sections of their stable and unstable manifolds must intersect. And such orbits must lie in the intersection. Note, these manifolds belong entirely to the Earth-Moon system and have nothing to do with the Sun-Earth system. But, in general, these intersections, if they exist, tend to be small, although not of measure zero. Arbitrarily picking points in the green ellipse will most likely result in a lunar capture orbit. A capture orbit is easily computed by trial and error. But, to be certain, one could use the algorithm developed in Koon et al (Ref. 1) and guarantee capture. Theoretically, a capture of any duration may be effected in this manner. In practice, a maneuver may be required for long-term capture.

5. End-to-End Trajectory Construction

To generate the end-to-end trajectory in the Bi-Circular model, select a point, Q, as in Figure 6. Integrate the Bi-Circular equations of motion backwards using Q as initial condition to obtain the launch trajectory. Integrate Q+ΔV forwards to obtain the lunar capture trajectory. Recall the ΔV is determined from the Jacobi constants of the two systems. This approach is completely analogous to the patch-conic technique. An initial trajectory is designed by patching conic arcs together. A differential corrector is used to move the conic arcs in phase space into an integrated trajectory from end-to-end using whatever ephemeris model is desired. In our case, instead of conic arcs, we are using arcs obtained from the invariant manifolds.

Figure 8.a is the final end-to-end trajectory integrated in the Bi-Circular model in inertial coordinates. A ΔV of 34 m/s is required at the location marked. Figure 8.b shows the same trajectory in Sun-Earth rotating frame. Note the characteristic loop at the lower right hand corner typical of insertions into halo or Lyapunov orbits. Clearly, the trajectory is following the stable manifold of the Lyapunov orbit, but doesn't have enough energy to capture onto the Lyapunov orbit and falls back to the Earth. But, as it falls back, it reaches the stable manifold of the Earth-Moon Lyapunov orbit. A small ΔV pushes it into a lunar capture orbit. Finally, Figure 8.c at the lower right hand corner shows the ballistic capture at the Moon in the Earth-Moon rotating frame.

Using the trajectory from the Bi-Circular model shown in Figure 8, an end-to-end trajectory has been computed in the JPL ephemeris model using JPL's LTool (Libration Point Mission Design Tool) currently under development. This computation is the subject of a future paper.

6. Conclusions

In this paper, we have laid bare the dynamical mechanism for Hiten-like lunar transfers and capture orbits. The role of dynamical systems theory, specifically the invariant manifold theory of periodic orbits about the Lagrange points, is crucial in the solution of this problem. In many of the previous applications of dynamical systems theory to mission design, the focus has been on using the trajectory arcs on the computed stable and unstable manifolds as initial guesses for the desired end-to-end trajectory. In the "Shoot the Moon" concept, we show that the tubular regions enclosed by the manifolds, the regions exterior to the manifolds, as well as the manifolds themselves all may be used to advantage depending on the desired characteristics of the final trajectory. The periodic orbits about the Lagrange points as well as their invariant manifolds provide an invaluable map of the different dynamical regimes in the phase space. Mission designers with this knowledge can pick and choose to their hearts' content, an infinite variety of trajectories to suit almost any purpose at hand. These objects, in a very real sense for missions in the delicate chaotic regions controlled by the Lagrange points, are the replacement of the wonderful porkchop plot handbooks generated by Andrey Sergeyevsky (Ref. 12 provides an example) that we have all come to depend on for conic-based mission design. As missions using the delicate dynamics of the Lagrange points become more wide spread, perhaps we should consider developing electronic handbooks to these chaotic regions of the Solar System.

To a great extent, our methodology depended on the fact that for the planar 3-body problem, the orbit space around the Lagrange points are completely classified by the Conley school. For the three dimensional 3-body problem, this is much more complex. Simo's school in Barcelona has made tremendous strides in classifying the orbits for this problem. But, the complete picture is still not known. The solution of this classification problem would have great impact on astrodynamics as well as planetary science and astronomy. Perhaps NASA and NSF could jointly support the development of this work in anticipation that somewhere in the next 30 years, the classification of orbits in the three-dimensional 3-body problem would provide another solution to an important space mission problem. Perhaps, it may provide a solution for an impending Near Earth Object in collision course with the Earth following the dynamical channels of the invariant manifolds. After all, this is how Shoemaker-Levy9 met its spectacular demise.

Acknowledgements

We thank James Miller and Edward Belbruno for useful discussions and advanced copies of papers. We thank Gerard Gomez and Josep Masdemont for many helpful discussions and for their wonderful software tools. We thank Paul Chodas for discussions on the SL9 and NEO orbits. We thank the LTool Team for the integrated trajectory with JPL ephemeris. We thank Aron Wolf for a careful review of of this paper.

This work was carried out at the Jet Propulsion Laboratory and California Institute of Technology under a contract with the National Aeronautics and Space Administration. This technology development was part of the LTool task which is supported by the JPL Technical Infrastructure Committee, the Telemetry and Mission Operations Directorate, the Center for Space Mission Architecture and Design, and the Genesis Mission. In addtion, this work was partially supported by the Caltech President's fund and NSF grant KDI/ATM-9873133.

References

1. Koon W.S., M. Lo, S. Ross, J. Marsden, Heteroclinic Connections between Liapunov Orbits and Resonance Transitions in Celestial Mechanics, to-appear in *Chaos*

2. Belbruno E., J. Miller, Sun-Perturbed Earth-to-Moon Transfers with Ballistic Capture, Journal of Guidance, Control and Dynamics 16, 1993, 770-775

3. Advances in Nonlinear Astrodynamics Conference, Nov. 8-10, 1993, The Geometry Center, Organizer: E. Belbruno

4. Belbruno, E.,The dynamical M3echanism of ballistic Lunar Cpature Transfers in the Four-Body Problem from the Perspective of Invariant Manifolds and Hill's Regions, Centre de Recerca matematica Preprint No. 270, 1994

5. Szebehely, V., Theory of Orbits, 1967, Academic Press, New York

6. Lo, M., and S. Ross, SURFing the Solar System: Invariant Manifolds and the Dynamics of the Solar System, JPL IOM 312/1997

7. Conley, C., Low Energy Transit Orbits in the Restricted Three-Body Problem, SIAM J. Appl. Math. 16, 1968, 732-746

8. McGehee R., Some Homoclinic Orbits for the Restricted Three Body Problem, Ph.D. Thesis, University of Wisconsin, 1969

9. Llibre J., R. Martinez, C. Simó, Transversality of the Invariant Manifolds Associated to the Lyapunov Family of Periodic Orbits Near L2 in the Restricted Three-Body Problem, Journal of Differential Equations 58, 1985, 104-156

10. Chodas P., D. Yeomans, The Orbital Motion and Impact Circumstances of Comet Shoemaker-Levy 9, in The Collision of Comet Shoemaker-Levy 9 and Jupiter, Edited by K.S. Noll, P.D. Feldman, and H.A. Weaver, Cambridge Unviersity Press, 1996

11. Koon, W.S., M. Lo, S. Ross, J. Marsden, The Genesis Trajectory and Heteroclinic Connections, AAS/AIAA Astrodynamics Specialist Conference, Girdwood, Alaska, 1999, AAS99-451

12. Sergeyevsky, A., and N. Lin, Interplanetary Mission Design Handbook, Volume 1, Part 1, JPL 82-43, Nov. 15, 1983

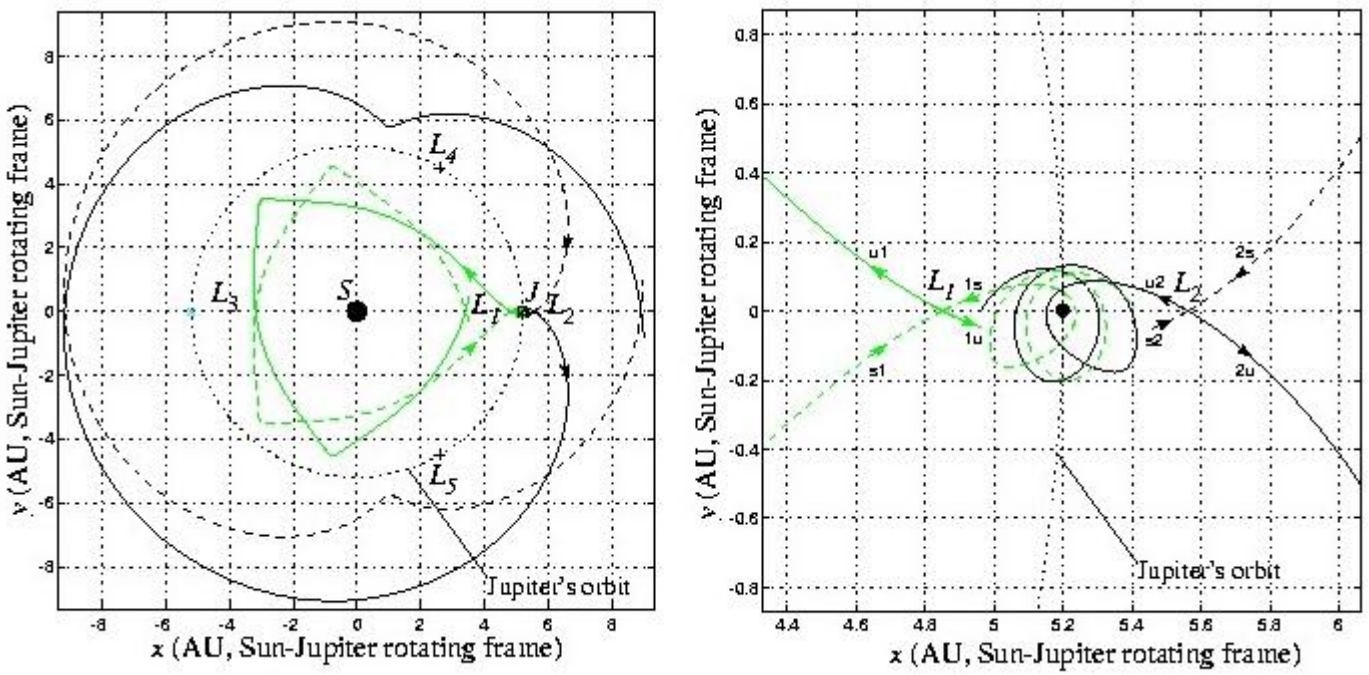

Figure 1. The 3 Body Problem in Rotating Frame. (Sun-Jupiter Case) The manifolds of the L1(green) and L2 (black) are shown. The stable manifold curve is dashed, the unstable manifold is solid.

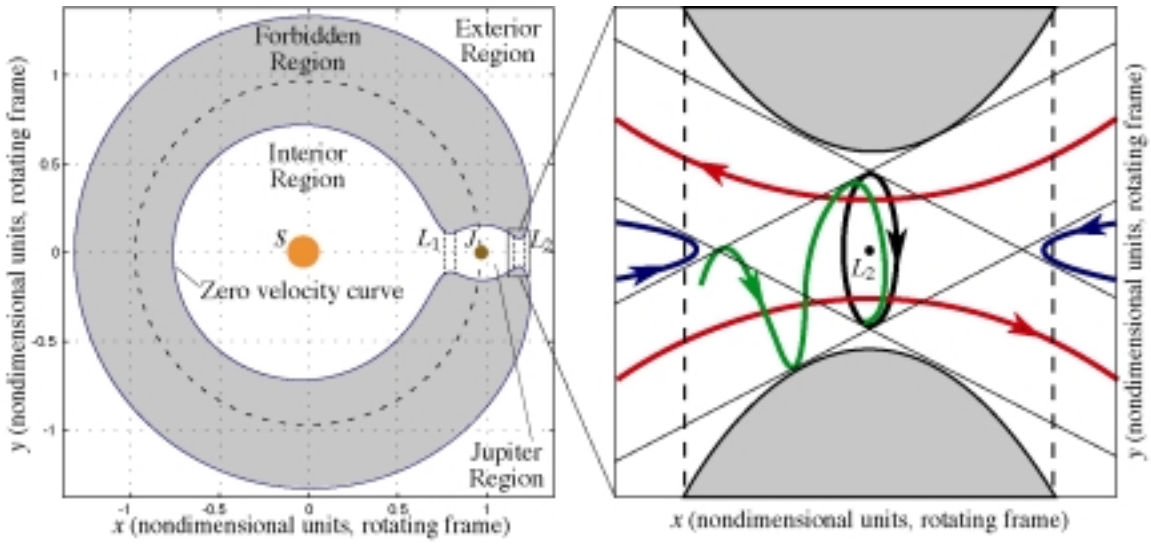

a. b.

Figure 2a. The Hill's Region Connecting the Interior (S), the Planet (J), and the Exterior (X) Regions.
2b. Expanded view of the L2 Region with 4 Major Classes of Orbits:
Black – Lyapunov Orbit (Unique for Each Energy Level)
Red – Transit Orbits (Must Pass Thru Lyapunov Orbit)
Green – Spiral Orbits (The Manifolds, Form Tubes),
Blue – Non-Transit Orbits.

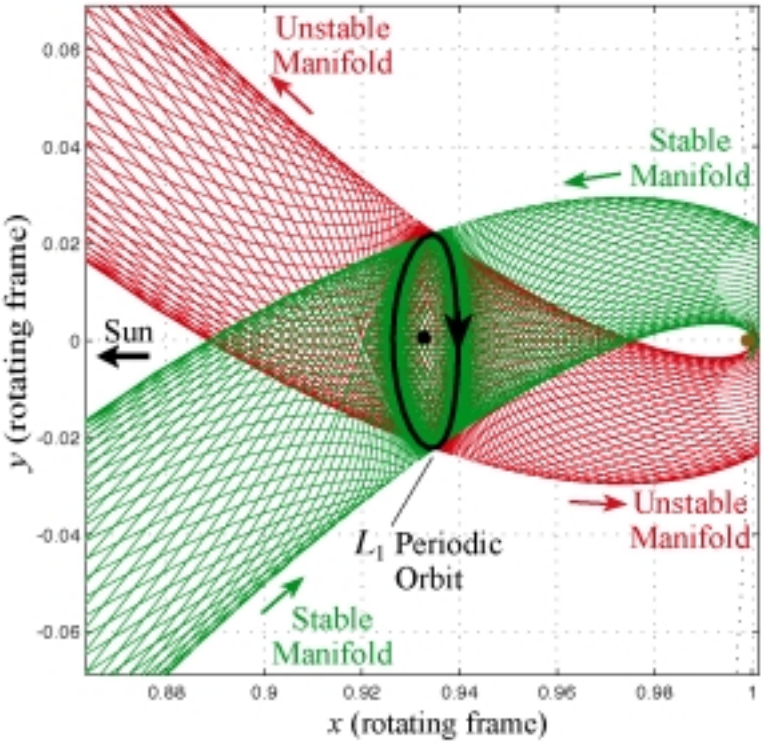

Figure 3. The Stable (Green) and Unstable (Red) Manifolds of a Lyapunov Orbit.

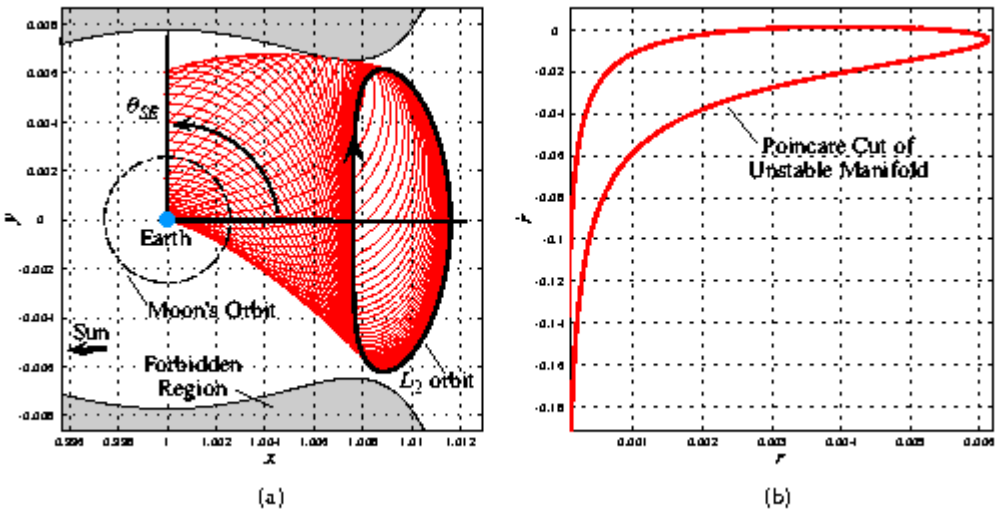

Figure 4. The Sun-Earth Unstable Manifold (Red) (a) and Its Poincare Section (b).

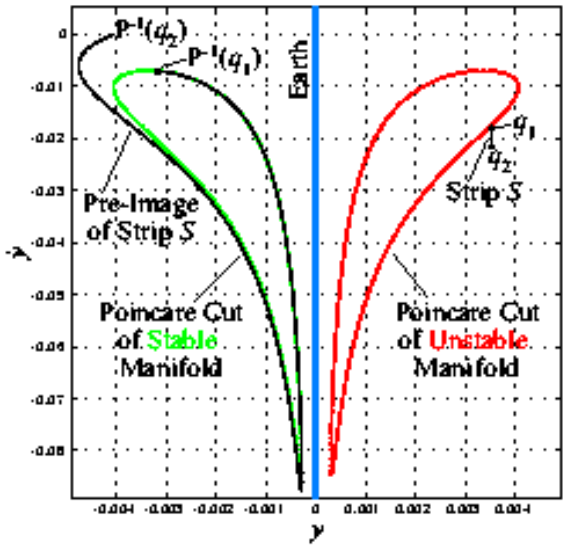

Figure 5. Using the Poincare Section to Find the Transfer Trajectory.

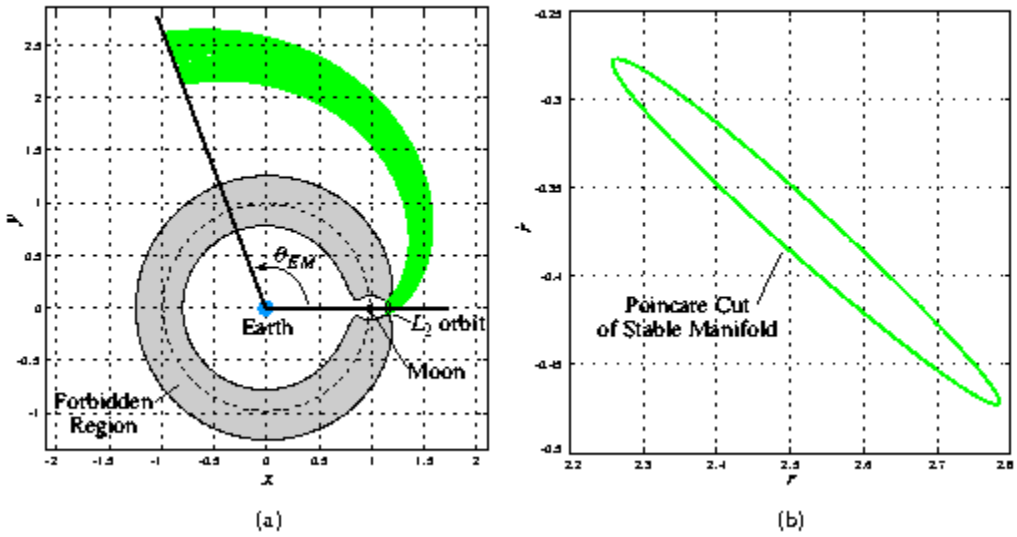

Figure 6. The Earth-Moon Unstable Manifold (Green) (a) and Its Poincare Section (b).

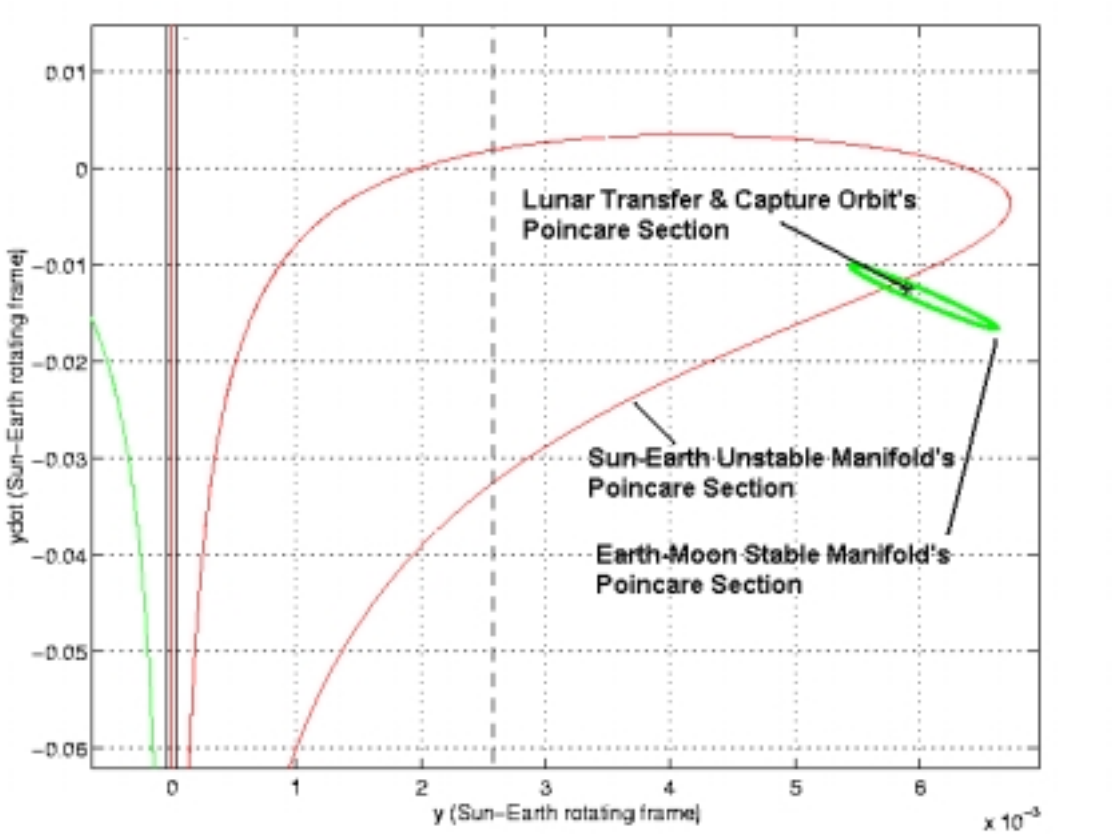

Figure 7. The Poincare Section of the Sun-Earth (Red) and Earth-Moon Unstable Manifold (Green).

Figure 8. Ballistic Capture by the Moon from a 200 km Earth Parking Orbit.
8.a Trajectory in Inertial Coordinates.

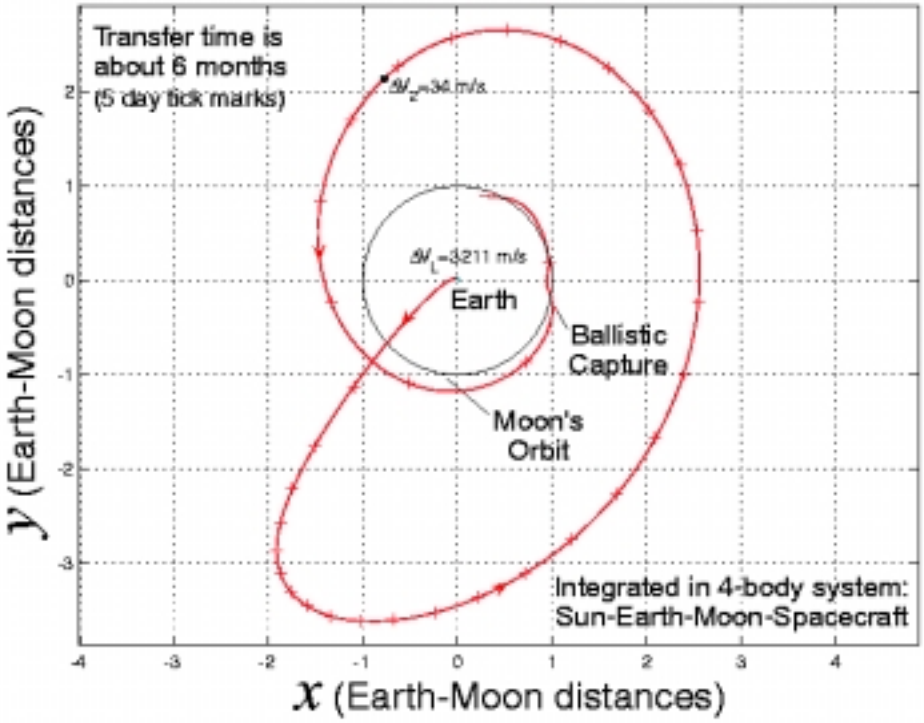

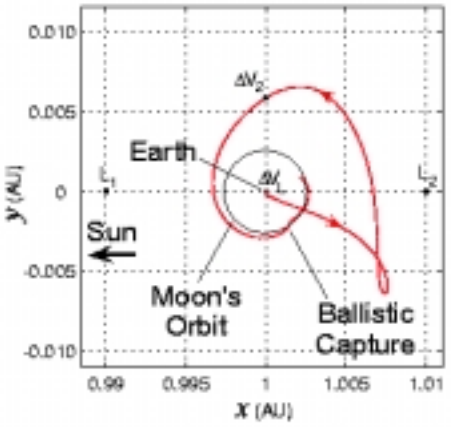

Figure 8.b Trajectory in Sun-Earth Rotating Frame.

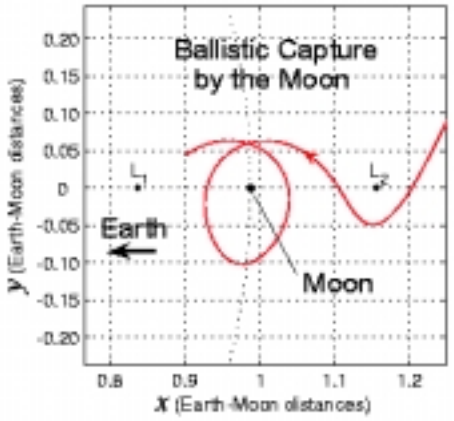

Figure 8.c Trajectory in Earth-Moon Rotating Frame.

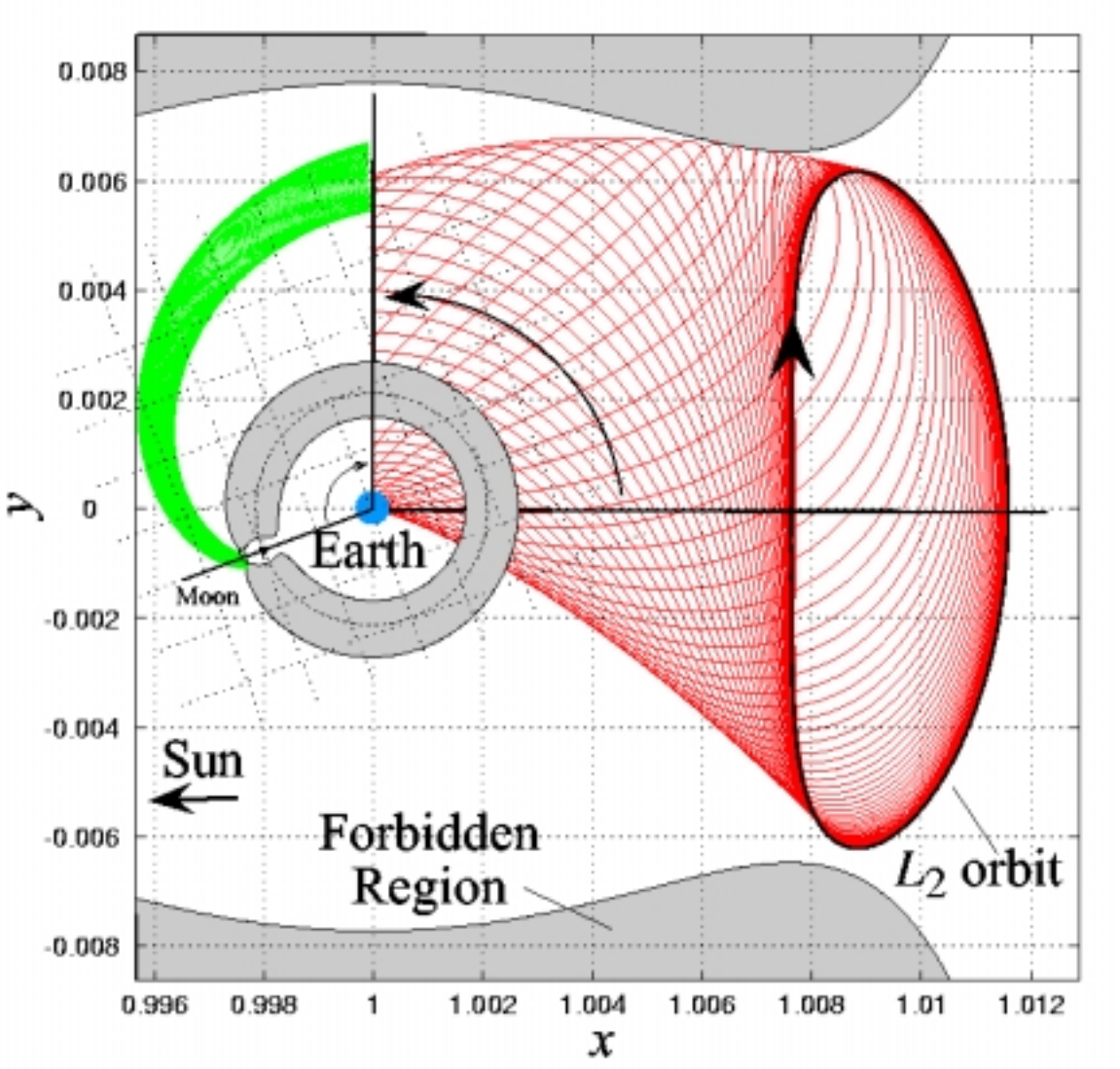
0.008
0.006
0.004
0.002
0
-0.002
-0.004
-0.006
-0.008
y
0.996
0.998
1
1.002
1.004
1.006
1.008
1.01
1.012
x
Earth
Moon
Sun
Forbidden
Region
L_2 orbit